I&EC research
Industrial & Engineering Chemistry Research

Article

pubs.acs.org/IECR

Mesoporous Carbons from Nanostructured Phenolic Thermosets Containing Poly(styrene-*alt*-maleic anhydride)-*block*-polystyrene Diblock Copolymer

Lei Li, Miaolin Huang, and Sixun Zheng*

Department of Polymer Science and Engineering and the State Key Laboratory of Metal Matrix Composites, Shanghai Jiao Tong University, Shanghai 200240, People's Republic of China

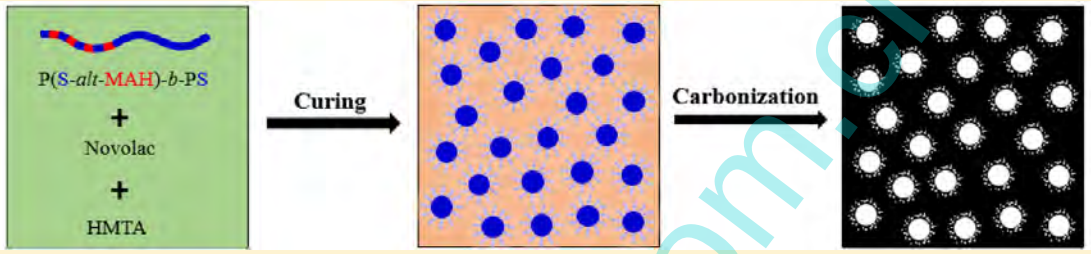

ABSTRACT: The nanostructured phenolic thermosets were prepared from the ternary mixtures composed of novolac resin, poly(styrene-*alt*-maleic anhydride)-*block*-polystyrene [P(S-*alt*-MAH)-*b*-PS] diblock copolymer, and hexamethylenetetramine, which were cured at elevated temperature. The P(S-*alt*-MAH)-*b*-PS diblock copolymer was synthesized via a one-pot RAFT polymerization approach. The morphologies of the nanostructured thermosets were modulated by changing the content of the diblock copolymer. The as-obtained nanostructured phenolic thermosets were further used as the precursors to obtain the mesoporous carbons via pyrolysis under highly pure nitrogen atmosphere. The mesoporous carbons were successfully obtained with adjustable porosity. The mesoporous carbons had specific surface areas of 398.9−491.4 $m^2\ g^{-1}$ and pore volumes of 0.22−0.31 $cm^3\ g^{-1}$.

INTRODUCTION

Highly porous carbons are a class of important materials which have applications in a variety of fields such as gas separation,[1,2] sorption catalysis,[3,4] and energy storage and conversion.[5,6] In terms of pore sizes, this class of materials can be classified into (i) microporous, (ii) mesoporous, and (iii) macroporous carbons.[7] Of them, considerable interest has been attracted to mesoporous carbons due to their large specific surface area and easily accessible pores. Generally, mesoporous carbons can be synthesized via so-called "hard-" and "soft-template" approaches.[8] For the hard-template approach, some inorganic templates such as silica[9−15] and alumina nanoparticles[16−18] are dispersed (or arranged) in the precursors of carbon. The resulting mesoporous carbons are then obtained via pyrolysis of the precursors. For the soft-template approach, amphiphilic molecules are incorporated into carbon precursors and the nanophases were then generated via a self-assembly mechanism. The size and morphologies of the self-assembled nanophases in the carbon precursors can be modulated with types, composition, and volume fractions of amphiphilic molecules in the carbon precursors. As a class of high-molecular-weight soft templates, amphiphilic block copolymers can be introduced to obtain the mesopores carbons with large nanopores.[19−30] In favorable cases, block copolymers themselves have been applied as the precursors of mesoporous carbons. For instance, the amphiphilic block copolymers containing polyacrylonitrile subchains can be directly carbonized into mesoporous carbons, the mesoporous structures of which can be modulated via self-assembled behavior of the block copolymers in bulk.[31−33] Alternatively, block copolymers can be regarded as soft templates to access the nanodomains in carbon precursors; the subsequent carbonization and pyrolysis of the nanostructured precursors would afford the mesoporous carbons.[34−38] Under this circumstance, it is required that the block copolymers contain the subchains which are miscible and immiscible with carbon precursors, respectively. The amphiphilicity of block copolymer is crucial to ensure the generation of the self-assembled nanostructure in carbon precursors.

Phenolic resins are a class of important thermosets for the production of adhesives, coatings, and electronic encapsulation materials.[39] Phenolic resins are also important precursors to obtain carbon materials with high yields.[40−42] In the past years, there have been a few reports on the synthesis of mesoporous carbons with nanostructured phenolic thermosets containing block copolymers as precursors. For instance, Zhao et al.[21,43−47] reported the formation of mesoporous carbons from mixtures of resol-type phenolic thermosets with poly(ethylene oxide)-*block*-polystyrene diblock copolymer and poly(ethylene oxide)-*block*-poly(propylene oxide)-*block*-poly(ethylene oxide) triblock

Received: August 9, 2016
Revised: October 15, 2016
Accepted: October 16, 2016
Published: October 27, 2016

DOI: 10.1021/acs.iecr.6b03048
Ind. Eng. Chem. Res. 2016, 55, 11502−11511

Scheme 1. Synthesis of P(S-*alt*-MAH)-*b*-PS Block Copolymer

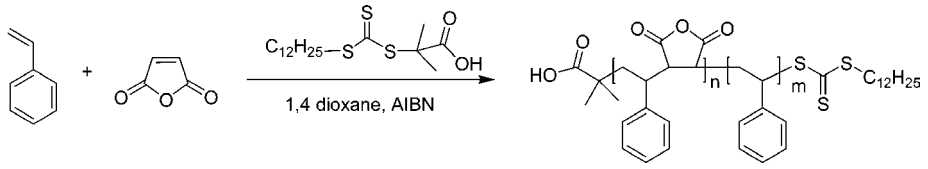

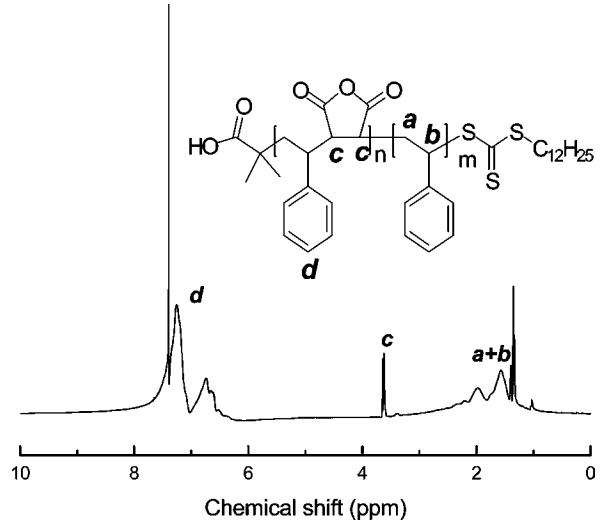

Figure 1. ^{1}H NMR spectrum of P(S-*alt*-MAH)-*b*-PS diblock copolymer in $CDCl_3$.

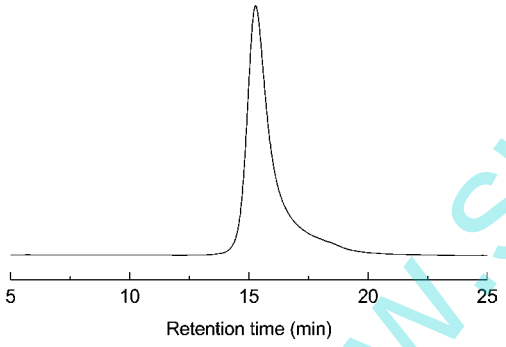

Figure 2. GPC curve of P(S-*alt*-MAH)-*b*-PS block copolymer.

copolymer. Ikkala et al.[36] reported the utilization of novolac-type phenolic thermosets to access mesoporous carbons with polystyrene-*block*-poly(4-vinylpyridine) diblock copolymer as the template. Zheng et al.[37] reported the preparation of mesoporous carbons from novolac resin and poly(ethylene oxide)-*block*-polystyrene diblock copolymer. By using poly(ethylene oxide)-*block*-(ε-caprolactone) diblock copolymer, Kuo et al.[48,49] also obtained nanoporous carbon with novolac-type phenolic thermosets as precursors. In all these previous works, the amphiphilic block copolymers contain the proton-accepting blocks such as poly(ethylene oxide) and poly(4-vinylpyrrolidine) or/and poly(2-vinylpyrrolidine), which were able to form hydrogen bonds with phenolic networks. The specific intermolecular reactions are critical to suppress the macroscopic phase separation in the multicomponent system.[31−49] Nonetheless, a question arises if such specific intermolecular interactions are required. If not, are there other interactions (e.g., inter-component chemical reaction[50]) which can be utilized to achieve this end? To the best of our knowledge, such an investigation remains largely unexplored.

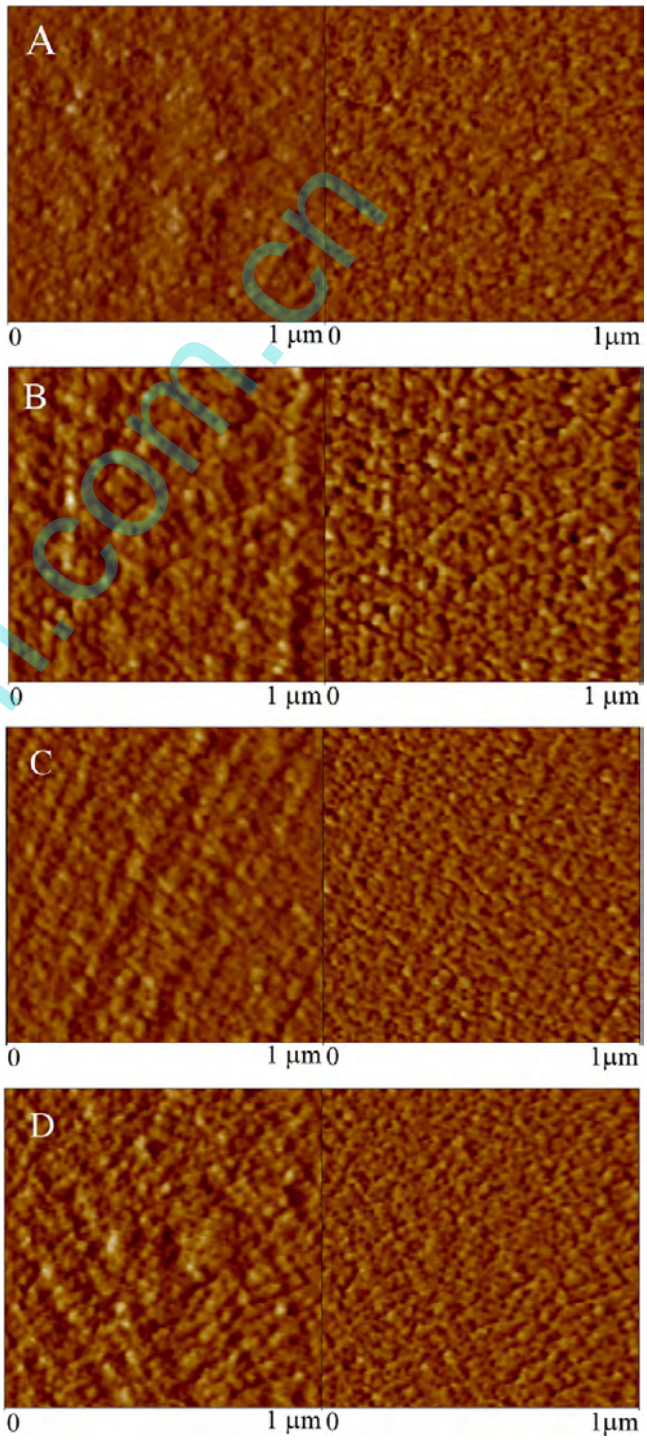

Figure 3. AFM micrographs of phenolic thermosets containing (A) 10, (B) 20, (C) 30, and (D) 40 wt % of P(S-*alt*-MAH)-*b*-PS diblock copolymer.

Herewith, we explored preparing nanostructured phenolic thermosets containing poly(styrene-*alt*-maleic anhydride)-*block*-polystyrene [P(S-*alt*-MAH)-*b*-PS], a novel diblock copolymer

DOI: 10.1021/acs.iecr.6b03048
Ind. Eng. Chem. Res. 2016, 55, 11502−11511

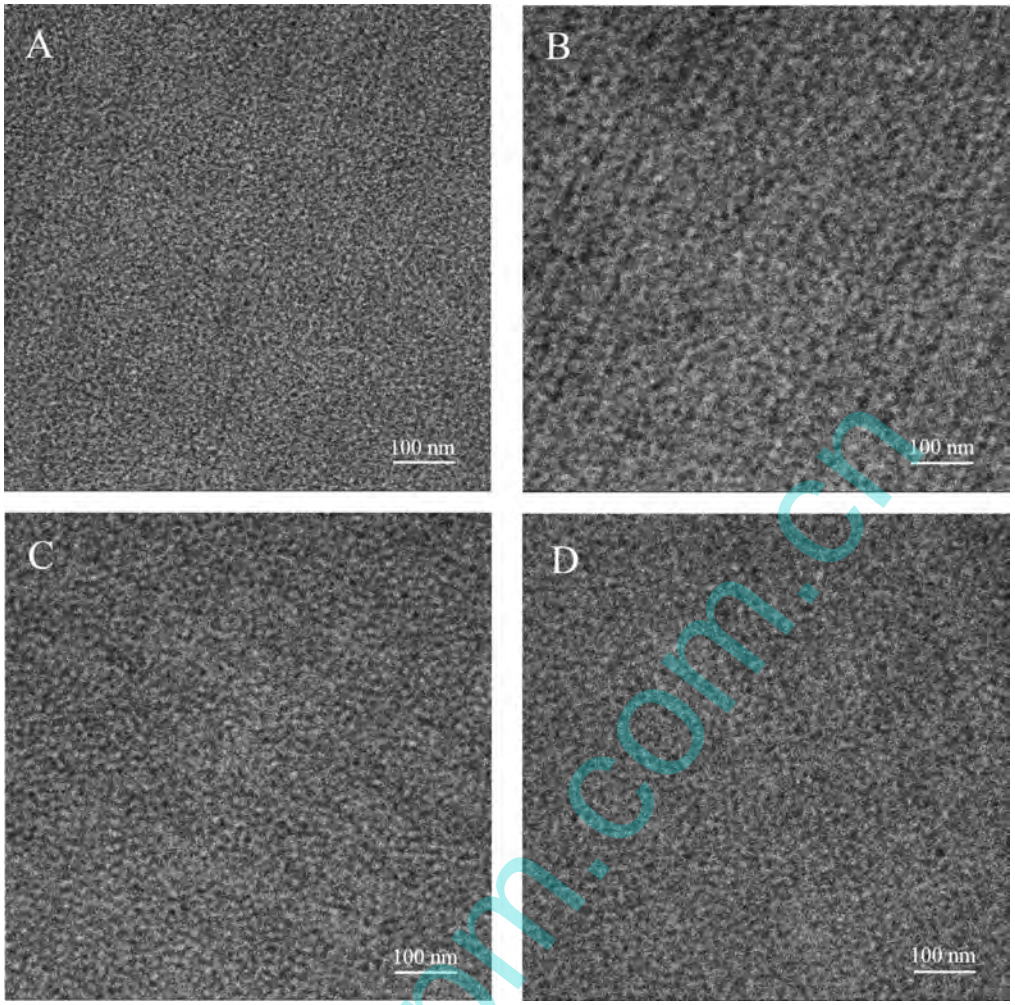

Figure 4. TEM micrographs of phenolic thermosets containing (A) 10, (B) 20, (C) 30, and (D) 40 wt % of P(S-*alt*-MAH)-*b*-PS diblock copolymer.

which is capable of reacting with phenolic networks. The nanostructured phenolic thermosets were then employed as precursors to access the mesoporous carbons. This block copolymer can be readily synthesized with a one-pot living radical polymerization approach.[51−53] It is expected that the intercomponent chemical linkages between the phenolic network and the P(S-*alt*-MAH) subchains would be formed via the intercomponent esterification between phenolic hydroxyl and anhydride groups. The intercomponent reaction can suppress the macroscopic phase separation of the diblock copolymer during the curing process. In this article, the morphologies of the nanostructured thermosets were modulated by changing the content of the diblock copolymer. The morphologies of the mesoporous carbons resulting from the thermosetting precursors have been characterized by using transmission electronic microscopy and small-angle X-ray scattering. Specific surface areas have been measured in terms of nitrogen absorption−desorption measurements.

EXPERIMENTAL SECTION

Materials. Novolac resin was kindly supplied by Rheine Chem. Co. Germany; it had a quoted molecular weight of M_n = 950 Da. 2-(Dodecylthiocarbonothioylthio)-2-methylpropanoic acid was synthesized by following literature methods.[54] Styrene (St), maleic anhydride (MAH), hexamethylenetetramine (HMTA), and azodiisobutyronitrile (AIBN) were purchased from Shanghai Reagent Co. China. The organic solvents such as 1,4-dioxane, petroleum ether, and dichloromethane were received from commercial sources.

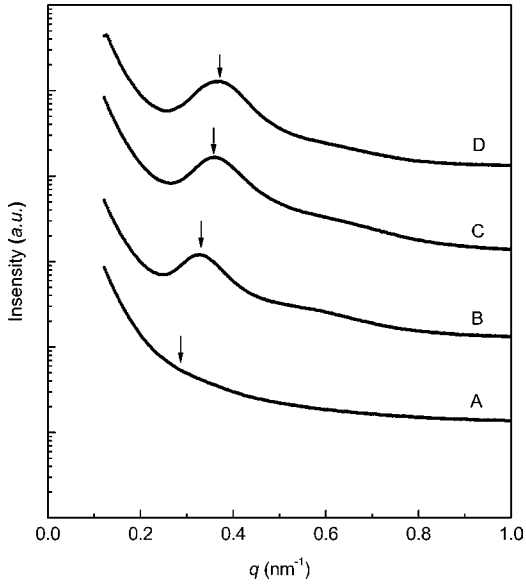

Figure 5. SAXS curves of phenolic thermosets phenolic thermosets containing (A) 10, (B) 20, (C) 30, and (D) 40 wt % of P(S-*alt*-MAH)-*b*-PS diblock copolymer.

DOI: 10.1021/acs.iecr.6b03048
Ind. Eng. Chem. Res. 2016, 55, 11502−11511

Synthesis of P(S-*alt*-MAH)-*b*-PS Diblock Copolymer. To a 25 mL flask, St (4.000 g, 38.5 mmol), MAH (0.500 g, 5.10 mmol), AIBN (8.200 mg, 0.05 mmol), and 2-(dodecylthiocarbonothioylthio)-2-methylpropanoic acid (0.072 g, 0.198 mmol) were dissolved in 5 mL of 1,4-dioxane. The mixture was purged with nitrogen for 45 min, and then the flask was immersed into an oil bath at 65 °C for polymerization for 24 h. Cooled to ambient temperature, 10 mL of 1,4-dioxane was added to dissolve the product. The solution was dropwise added into 100 mL of petroleum ether to obtain the precipitates. After being dried in vacuo at 25 °C for 24 h, diblock copolymer (3.000 g) was obtained with a yield of 66.7%. ^{1}H NMR ($CDCl_3$, ppm): 7.10−7.26 (50H, protons of phenyl groups); 3.68 (2H, −C***H***C***H***−); 1.10−2.10 (15H, −C***H***$_2$− and −C***H***(C_6H_5)− in the backbone of PS chain). GPC: M_n = 15 000 Da with M_w/M_n = 1.10.

Preparation of Phenolic Thermosets. Typically, P(S-*alt*-MAH)-*b*-PS diblock copolymer (0.400 g) and novolac (3.300g) were dissolved in dichloromethane (5 mL) at room temperature, and then HMTA (0.330g) dissolved in 2 mL of dichloromethane was added to the mixture; the mixture was agitated for 30 min. The majority of solvents were removed via evaporation at ambient temperature overnight; the residual solvents were then eliminated in vacuo at 60 °C for 4 h. The mixture was transferred to aluminum foil, and they were cured at 100 °C for 2 h, 150 °C for 2 h, and 190 °C for an additional 30 min.

Preparation of Mesoporous Carbons. The above phenolic thermosets were carbonized in a tube furnace at elevated temperature. In a highly pure nitrogen atmosphere, the thermosets were first heated to 150 °C and maintained at 150 °C for 30 min. Thereafter, the temperature of the furnace was enhanced to 450 °C at a rate of 2 °C min^{-1} and maintained at 450 °C for 3 h. After that the temperature was further increased to 600 °C at a rate of 1 °C min^{-1}. Finally, the temperature was enhanced to 800 °C at a rate of 5 °C min^{-1}; the samples were maintained at 800 °C for 7 h to attain complete carbonization.

Measurements and Characterization. Proton nuclear magnetic resonance (^{1}H NMR) spectroscopy was conducted on a Bruker AVANCE III HD 400 spectrometer. Gel permeation chromatography (GPC) was conducted on a DAWN EOS apparatus equipped with three styragel columns; THF was used as the eluent. Infrared spectroscopy was conducted on a PerkinElmer Paragon 1000 FTIR spectrometer. The samples were ground and mixed with potassium bromide pellets, and the mixtures were then pressed into thin flakes. Atomic force microscopy (AFM) was performed on a CSPM 5500 atomic force microscope operating with a tapping mode. Silicon probes with a length of 125 μm and a resonant frequency of ca. 300 kHz were used for the measurements. The morphologies were observed on a JEOL JEM-2010 transmission electron microscope operating at 120 kV. The phenolic thermosets were sliced into ultrathin sections with a thickness of ca. 70 nm. To increase the difference in electron density, the sections were stained with RuO_4. To observe the morphologies of mesoporous carbons, the carbons were first grounded and the powder was dispersed in ethanol via sonication; the suspensions were dropped on copper grids, and then the solvent was removed before the measurements. The SAXS experiments were conducted on the BL16B station of Shanghai Synchrotron Radiation Facility.[55] Nitrogen sorption and desorption measurements were carried out on an ASAP 2010 gas sorption analyzer at 77 K on the basis of Brunauer−Emmett−Teller (BET) measurements. Pore size distribution was examined with the nonlocal density functional theory (NLDFT) method.

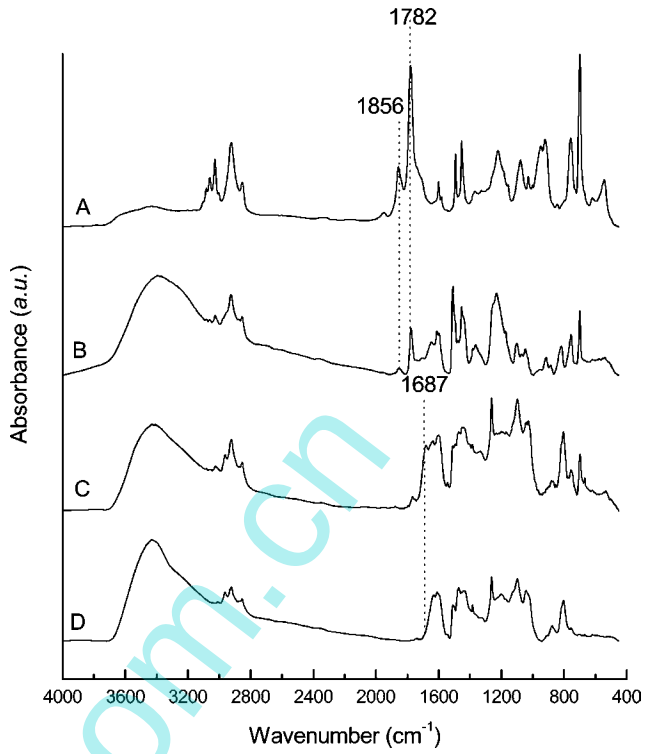

Figure 6. FTIR spectra of (A) P(S-*alt*-MAH)-*b*-PS block copolymer, (B) the mixture of novolac, HMTA, and 30 wt % of P(S-*alt*-MAH)-*b*-PS at room temperature, (C) the phenolic thermoset containing 30 wt % of P(S-*alt*-MAH)-*b*-PS diblock copolymer, and (D) novolac resin.

RESULTS AND DISCUSSION

Synthesis of P(S-*alt*-MAH)-*b*-PS Diblock Copolymer. The synthesis of P(S-*alt*-MAH)-*b*-PS diblock copolymer is depicted in Scheme 1. A one-pot route via RAFT polymerization was employed to obtain the diblock copolymer. It has been realized that the pair of St and MAH monomers can form a typical charge transfer complex (CTC).[56] The CTC formation is readily utilized to obtain P(S-*alt*-MAH) alternating copolymer via a conventional free radical polymerization, while the molar ratio of maleic anhydride to styrene was 1:1.[56−58] On the same principle, a P(S-*alt*-MAH)-*b*-PS diblock copolymer can be prepared while styrene was in excess and a living radical polymerization was carried out.[51−53] In this work, we synthesized a P(S-*alt*-MAH)-*b*-PS diblock copolymer with a one-pot RAFT polymerization approach. The polymerization was carried out with 2-(dodecylthiocarbonothioylthio)-2-methylpropanoic acid as the chain transfer agent and AIBN as the initiator; the feed molar ratio of MAH to St was fixed at 1:7.5 to afford a diblock copolymer with the desired mass fraction of PS subchain. Figure 1 shows the ^{1}H NMR spectrum of P(S-*alt*-MAH)-*b*-PS diblock copolymer. The resonance peaks appearing at 1.58, 1.84, and 7.10−7.26 ppm are attributed to the protons of the methylene, methine, and phenyl groups in PS block, respectively. The resonance peak at 3.68 ppm is attributed to the protons of the methine group of maleic moiety in P(S-*alt*-MAH) block. According to the integral ratio of methine protons of PMAH to phenyl protons of PS, the mass ratio of P(S-*alt*-MAH)] to PS block was estimated to about be 1:4. The molecular weight of P(S-*alt*-MAH)-*b*-PS diblock copolymer was measured by GPC (see Figure 2). This diblock copolymer had a molecular weight of M_n = 15 000 with M_w/M_n = 1.10. The ^{1}H NMR and GPC results are indicative

DOI: 10.1021/acs.iecr.6b03048
Ind. Eng. Chem. Res. 2016, 55, 11502−11511

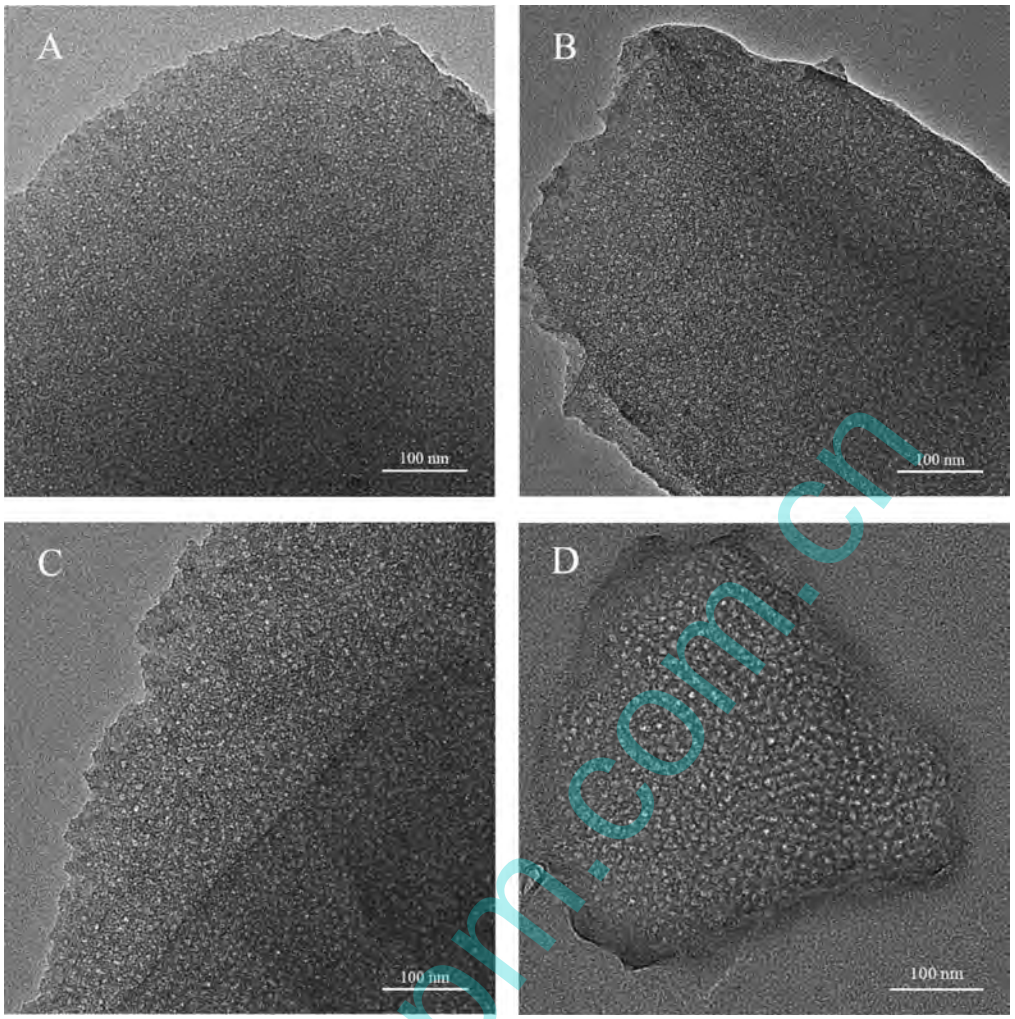

Figure 7. TEM micrographs of the mesoporous carbons from the phenolic thermosets containing (A) 10, (B) 20, (C) 30, and (D) 40 wt % of P(S-*alt*-MAH)-*b*-PS.

of the successful synthesis of P(S-*alt*-MAH)-*b*-PS diblock copolymer.

Nanostructured Phenolic Thermosets. The mixtures composed of novolac, P(S-*alt*-MAH)-*b*-PS diblock copolymer, and HMTA at 10 wt % with respect of novolac resin were cured. By controlling the mass ratios, the phenolic thermosets were prepared with contents of block copolymer up to 40 wt %. All the phenolic thermosets containing P(S-*alt*-MAH)-*b*-PS were transparent and homogeneous, suggesting that no macroscopic phase separation occurred. The morphologies of the as-synthesized phenolic thermosets containing P(S-*alt*-MAH)-*b*-PS were studied by AFM, TEM, and SAXS. Figure 3 shows AFM micrographs of the phenolic thermosets with different contents of P(S-*alt*-MAH)-*b*-PS. In the AFM micrographs, the height and phase shift images were in the left- and right-hand sides, respectively. From height images, it is seen that the surfaces of the sections were quite flat and smooth. Therefore, the phase shift images would reflect the phase separation behavior. The phase shift images showed that all phenolic thermosets displayed microphase-separated structure. In terms of the content of P(S-*alt*-MAH)-*b*-PS in the thermosets and the difference in viscoelastic properties between PS and phenolic matrix, it is judged that the dark domains resulted from the PS blocks whereas the light regions were attributable to the phenolic matrix which remained mixed with the P(S-*alt*-MAH) block. The microphase-separated morphologies were further demonstrated by TEM measurements (See Figure 4). To increase the difference in electron density, the specimens were stained with RuO_4. In this case, phenolic matrix can be stained whereas the PS microdomains remained unvaried. Therefore, the dark region in the TEM micrographs are responsible for phenolic matrices whereas the light to PS microdomains. Notably, the spherical and/or worm-like PS nanophases with a diameter of 10−30 nm were homogeneously dispersed into phenolic matrices. The number of the PS microdomains increased as the content of P(S-*alt*-MAH)-*b*-PS diblock copolymer increased.

The nanostructured phenolic thermosets were further subjected to SAXS; the SAXS curves are presented in Figure 5. All the thermosets displayed the scattering phenomena, suggesting that the phenolic thermosets containing P(S-*alt*-MAH)-*b*-PS were indeed microphase-separated. The scattering intensity increased with the percentage of P(S-*alt*-MAH)-*b*-PS in the phenolic thermosets. As the content of P(S-*alt*-MAH)-*b*-PS increased, the primary scattering peaks of SAXS curves shifted to the higher q positions, suggesting that the distances among the adjacent microdomains were significantly decreased. This result was in accordance with the observations from AFM and TEM. These morphological results indicate that the nanostructured phenolic thermosets were successfully obtained.

DOI: 10.1021/acs.iecr.6b03048
Ind. Eng. Chem. Res. 2016, 55, 11502−11511

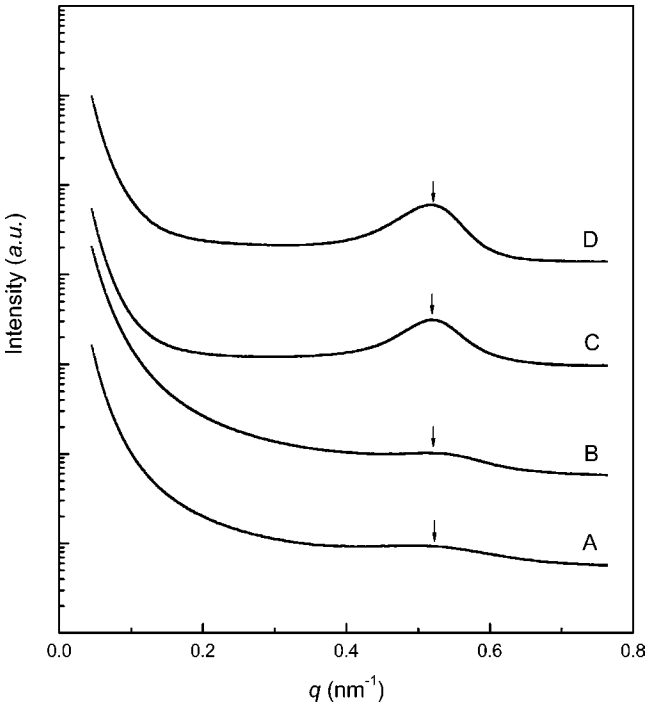

Figure 8. SAXS curves of the mesoporous carbon from the phenolic thermosets containing (A) 20, (B) 20, (C) 30, and (D) 40 wt % of P(S-*alt*-MAH)-*b*-PS diblock copolymer.

It is judged that in the nanostructured thermosets PS blocks were segregated from phenolic matrix to form the isolated microdomains and P(S-*alt*-MAH) block remained mixed with the phenolic networks. The intimate mixing of P(S-*alt*-MAH) blocks with phenolic matrix is attributable to the intercomponent esterification between phenolic hydroxyl groups of phenolic network and anhydride groups of P(S-*alt*-MAH) block at elevated temperature. This reaction was readily confirmed by FTIR spectroscopy. Figure 6 shows the FTIR spectra of P(S-*alt*-MAH)-*b*-PS, the mixture of the phenolic precursors (viz. novolac + HMTA) with 30 wt % of P(S-*alt*-MAH)-*b*-PS before the curing reaction, the cured blends, and novolac resin. For P(S-*alt*-MAH)-*b*-PS (see curve A), the characteristic bands at 1782 and 1856 cm^{-1} are assignable to the symmetric and asymmetric stretching vibration of anhydride carbonyl groups.[59] For the blends of the phenolic precursors (viz. novolac + HMTA) with the diblock copolymer (30 wt %), these two bands were also discernible (see curve B). After the mixture was cured at elevated temperature, both of the bands completely disappeared; concurrently a new band at 1687 cm^{-1} appeared, responsible for the stretching vibration of ester carbonyl groups (see curve C). FTIR spectroscopy indicates that covalent bonds were indeed formed between phenolic matrix and P(S-*alt*-MAH) of the diblock copolymer.

Mesoporous Carbons. The nanostructured phenolic thermosets containing P(S-*alt*-MAH)-*b*-PS were used as the precursors, which were then carbonized at a temperature as high as 800 °C, to obtain the mesoporous carbons. In the process of pyrolysis, the PS microdomains would be eliminated, leaving the nanopores, whereas the matrices composed of phenolic network and P(S-*alt*-MAH) would be carbonized into carbons. The morphologies of the resulting carbons were examined by using TEM and the TEM micrographs are shown in Figure 7. Notably, all samples displayed the heterogeneous morphologies. It should be pointed out that the TEM specimens were prepared without staining steps. According to the difference in electron density, the light and spherical (or worm-like) features are attributed to the nanopores formed due to the removal of the PS microdomains in the process of carbonization whereas the dark regions to the carbon matrices from the carbonization of the phenolic matrices. It is noted that in all cases nanopores with a diameter of 10−20 nm were formed. It is observed that the number and size of the nanopores increased with the content of P(S-*alt*-MAH)-*b*-PS in the phenolic thermosets. As the content of diblock copolymer in the thermosets was 40 wt % (i.e., the content of PS block was 32 wt %), the nanopores became interconnected, i.e., some worm-like (or cylindrical) nanopores were generated.

The mesoporous carbons were subjected to SAXS and SAXS curves as presented in Figure 8. In all cases, scattering phenomena were exhibited, which indicated that the nanopores were indeed formed. The scattering intensity increased with the concentration of P(S-*alt*-MAH)-*b*-PS in the thermosets. Compared to the corresponding phenolic thermosets, the SAXS profiles of the mesoporous carbons displayed the following features: (i) the primary scattering peaks shifted to the higher q value position and (ii) all scattering peaks were constantly at a values of q_m= 0.52 nm^{-1}, in marked contrast to the observation that the primary peaks increasingly shifted to higher q positions with the increase of the content P(S-*alt*-MAH)-*b*-PS diblock copolymer in the thermosets. In comparison with the nanostructured phenolic thermosets containing P(S-*alt*-MAH)-*b*-PS, there could be the following changes involved with the formation of the mesopores in the carbon materials. First, the volume shrinkage induced by carbonization would occur due to the removal of the labile components (i.e., oxygen and hydrogen elements). This change resulted that the average distance between the adjacent nanopores in the mesoporous carbon was smaller than that between the PS microdomains in the phenolic thermoset. As a consequence, the long period in the mesoporous carbons was smaller than those in the corresponding nanostructured thermosets. Second, the size of the nanopores in the carbon materials could be larger than that of the PS microdomains in the phenolic matrix. In the nanostructured thermosets, the P(S-*alt*-MAH) blocks were intimately mixed

Scheme 2. Preparation of Mesoporous Carbon

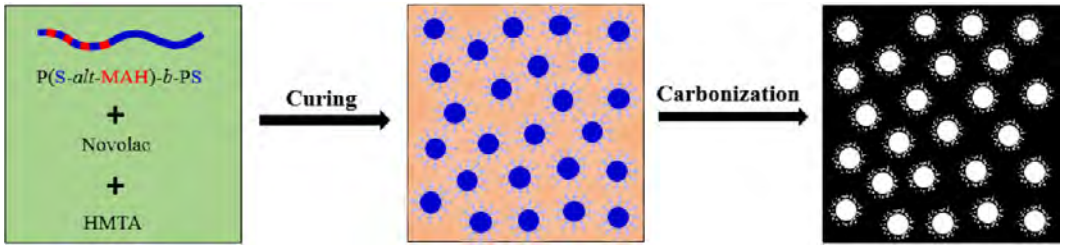

DOI: 10.1021/acs.iecr.6b03048
Ind. Eng. Chem. Res. 2016, 55, 11502−11511

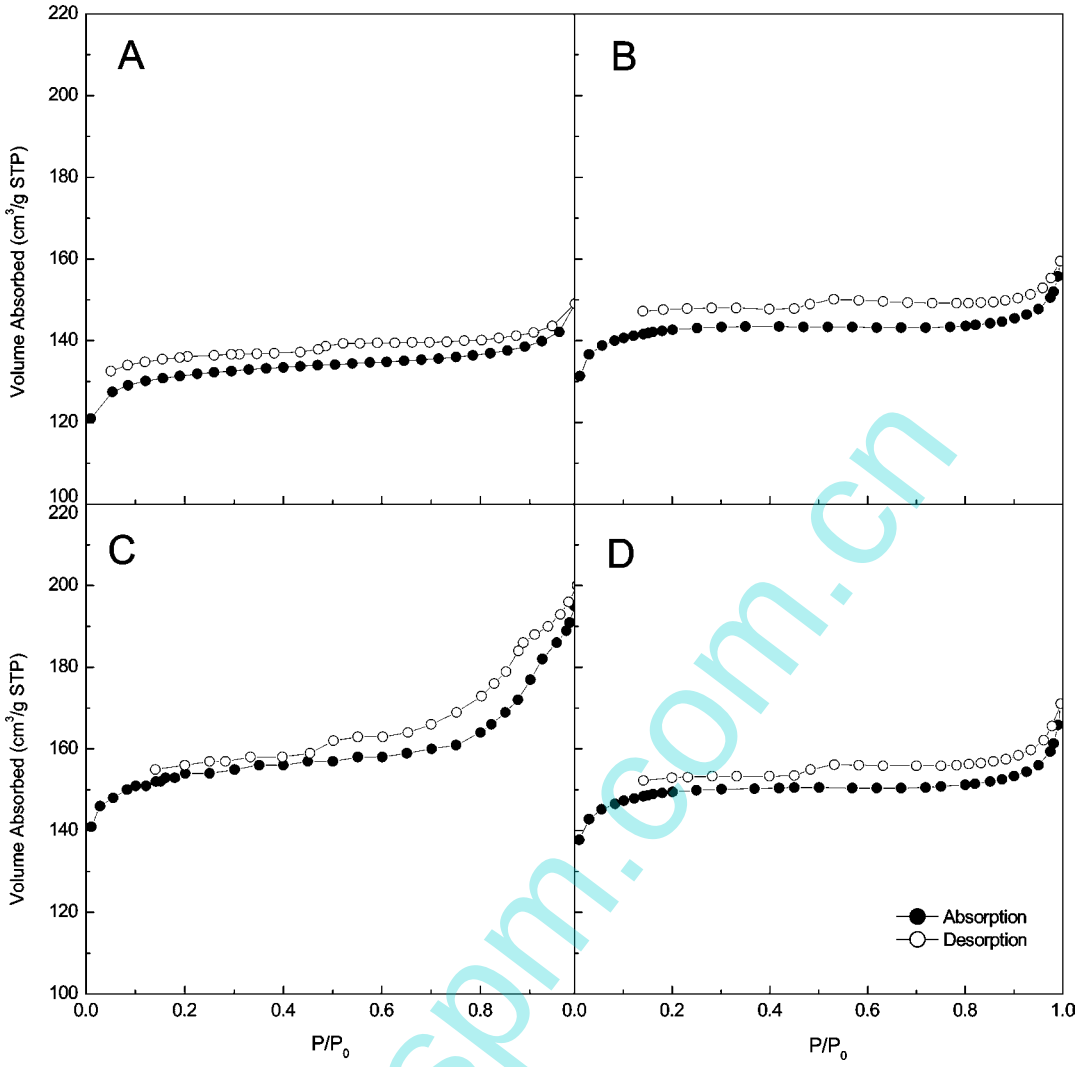

Figure 9. Nitrogen sorption and desorption isotherms of the mesoporous carbons from the phenolic thermosets containing (A) 10, (B) 20, (C) 30, and (D) 40 wt % of P(S-*alt*-MAH)-*b*-PS diblock copolymer.

with phenolic networks and around the PS microdomains owing to their chemical linkage with PS blocks. The pyrolysis of these P(S-*alt*-MAH) blocks left a great number of micropores around nanopores (see Scheme 2). It is proposed that the size of the resulting nanopores would encompass the contribution from this portion of micropores. The increase in sizes of nanopores can be reflected in the decrease in long period in the SAXS measurement. In addition, the nanopores could become interconnected owing to the formation of the microdomains around the nanopores, especially when the concentration of PS block was very high (e.g., 32 wt %) (see Figure 7D). The interconnected (or worm-like) nanopores in the carbon matrix would display a form factor scattering different from the spherical PS microdomains.

The above mesoporous carbons were subjected to nitrogen sorption−desorption experiments; the nitrogen sorption−desorption isotherms are shown in Figure 9. All mesoporous carbons displayed type-IV isotherms and a H2-type hysteresis loop; meanwhile, the capillary condensation phenomena appeared at the higher P/P_0 region (e.g., $P/P_0 > 0.9$). This observation suggests that cage-like nanopores with small windows (i.e., micropores) in the walls existed. It is proposed that the nanopores resulted from removal of the PS microdomains, whereas the micropores were from the pyrolysis of P(S-*alt*-MAH) blocks in the surrounding of the the PS microdomains. The specific surface areas were calculated to be 398.9, 452.9, 491.4, and 474.7 $m^2\ g^{-1}$ for the mesoporous carbons from the thermosets with contents of P(S-*alt*-MAH)-*b*-PS 10, 20, 30, and 40 wt %, respectively. The corresponding pore volumes were 0.22, 0.25, 0.31, and 0.26 $cm^3\ g^{-1}$, respectively (Table 1). It is found that the values of the specific surface area and pore volume increased with the content of diblock copolymer in the thermosets. Notably, both values of the carbon from the thermoset containing 40 wt % of P(S-*alt*-MAH)-*b*-PS were lower than that of the mesoporous

Table 1. Pore Volume and Surface Area of Mesoporous Carbon Materials

samples[a]	concentration of block copolymer (wt %)	concentration of PS block (wt %)	pore volume (cm^3/g)	surface area (cm^2/g)
MC1	10	8	0.22	398.9
MC2	20	16	0.25	452.9
MC3	30	24	0.31	491.4
MC4	40	32	0.26	474.7

[a]MC1, MC2, MC3, and MC4 stand for the mesoporous carbons from the phenolic thermosets containing P(S-*alt*-MAH)-*b*-PS diblock copolymer.

DOI: 10.1021/acs.iecr.6b03048
Ind. Eng. Chem. Res. 2016, 55, 11502−11511

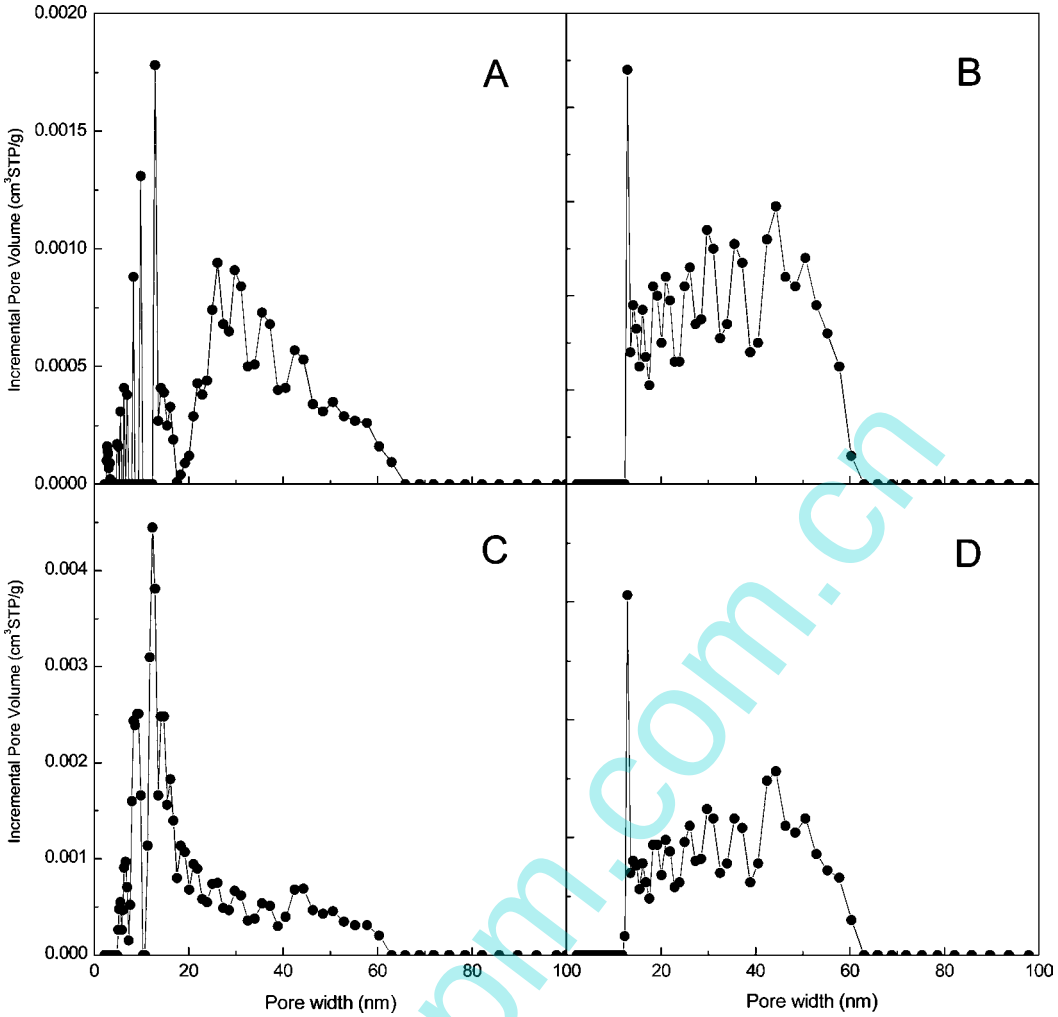

Figure 10. Incremental pore volume distribution data obtained by fitting the NLDFT model to sorption isotherms for the mesoporous carbons from the phenolic thermosets containing (A) 10, (B) 20, (C) 30, and (D) 40 wt % of P(S-*alt*-MAH)-*b*-PS diblock copolymer.

carbons from the thermoset containing 30 wt % of P(S-*alt*-MAH)-*b*-PS. This observation could be interpreted as the formation of a great number of worm-like (or cylindrical) nanopores in the carbon.

In this work, the pore size distributions of the mesoporous carbons were analyzed using the NLDFT method[60−62] since the pore sizes were beyond the range of micromesopores. Figure 10 shows plots of incremental pore volumes of the mesoporous carbons as a function of the pore width. Notably, the pore volumes of all mesoporous carbons displayed a broad distribution. Some pores had a width of 20−40 nm, whereas others were smaller than 10 nm in width. The larger pores could be generated with pyrolysis of the PS microdomains in the thermosets, whereas pores with a smaller width were attributable to the microdomains resulting from pyrolysis of the matrix (Scheme 2). It should be pointed out that the values of the pore width according to NLDFT were different from those from TEM owing to the methodological difference in the measurement of pore volumes.[60−62] Nonetheless, the results of the nitrogen sorption-desorption measurements indicate that the mesoporous carbons with adjustable porosity were successfully obtained.

■ CONCLUSIONS

Mesoporous carbons were successfully prepared from the nanostructured phenolic thermosets containing [P(S-*alt*-MAH)-*b*-PS], a new block copolymer. The nanostructured phenolic thermosets were prepared from ternary mixtures composed of novolac resin, poly(styrene-*alt*-maleic anhydride)-*block*-polystyrene [P(S-*alt*-MAH)-*b*-PS] diblock copolymer, and hexamethylenetetramine, which were cured at elevated temperature. In the thermosets, PS homopolymer subchains were segregated from phenolic matrix as the PS microdomains whereas the P(S-*alt*-MAH) blocks remained mixed with the phenolic matrix owing to formation of the covalent bonds via esterification between phenolic hydroxyl groups of the phenolic network and anhydride groups of the P(S-*alt*-MAH) block. The nanostructured phenolic thermosets were successfully carbonized into the mesoporous carbon. Depending on the composition of the nanostructured phenolic thermosets, mesoporous carbons with adjustable porosity were successfully obtained.

■ AUTHOR INFORMATION

Corresponding Author

*Tel.: 86-21-54743278. Fax: 86-21-54741297. E-mail: szheng@sjtu.edu.cn.

Notes

The authors declare no competing financial interest.

DOI: 10.1021/acs.iecr.6b03048
Ind. Eng. Chem. Res. 2016, 55, 11502−11511

■ ACKNOWLEDGMENTS

The authors are thankful for financial support from the National Natural Science Foundation of China (Nos. 51133003, 21304058, and 21274091). The projects (Nos. 10sr0260 and 10sr0126) in the Shanghai Synchrotron Radiation Facility are gratefully acknowledged.

■ REFERENCES

(1) Ismail, A. F.; David, L. I. B. A Review on the Latest Development of Carbon Membranes for Gas Separation. *J. Membr. Sci.* **2001**, *193*, 1−18.
(2) Mahurin, S. M.; Lee, J. S.; Wang, X.; Dai, S. Ammonia-Activated Mesoporous Carbon Membranes for Gas Separations. *J. Membr. Sci.* **2011**, *368*, 41−47.
(3) Shanahan, P. V.; Xu, L.; Liang, C.; Waje, M.; Dai, S.; Yan, Y. Graphitic Mesoporous Carbon as a Durable Fuel Cell Catalyst Support. *J. Power Sources* **2008**, *185*, 423−427.
(4) Hartmann, M.; Vinu, A.; Chandrasekar, G. Adsorption of Vitamin E on Mesoporous Carbon Molecular Sieves. *Chem. Mater.* **2005**, *17*, 829−833.
(5) Candelaria, S. L.; Shao, Y.; Zhou, W.; Li, X.; Xiao, J.; Zhang, J.; Wang, Y.; Liu, J.; Li, J.; Cao, G. Nanostructured Carbon for Energy Storage and Conversion. *Nano Energy* **2012**, *1*, 195−220.
(6) Yang, Z.; Ren, J.; Zhang, Z.; Chen, X.; Guan, G.; Qiu, L.; Zhang, Y.; Peng, H. Recent Advancement of Nanostructured Carbon for Energy Applications. *Chem. Rev.* **2015**, *115*, 5159−5223.
(7) Lee, J.; Kim, J.; Hyeon, T. Recent Progress in the Synthesis of Porous Carbon Materials. *Adv. Mater.* **2006**, *18*, 2073−2094.
(8) Liang, C.; Li, Z.; Dai, S. Mesoporous Carbon Materials: Synthesis and Modification. *Angew. Chem., Int. Ed.* **2008**, *47*, 3696−3717.
(9) Wu, C.; Bein, T. Conducting Carbon Wires in Ordered, Nanometer-Sized Channels. *Science* **1994**, *266*, 1013−1015.
(10) Ryoo, R.; Joo, S. H.; Jun, S. Synthesis of Highly Ordered Carbon Molecular Sieves *via* Template-Mediated Structural Transformation. *J. Phys. Chem. B* **1999**, *103*, 7743−7746.
(11) Jun, S.; Joo, S. H.; Ryoo, R.; Kruk, M.; Jaroniec, M.; Liu, Z.; Ohsuna, T.; Terasaki, O. Synthesis of New, Nanoporous Carbon with Hexagonally Ordered Mesostructure. *J. Am. Chem. Soc.* **2000**, *122*, 10712−10713.
(12) Yu, C.; Fan, J.; Tian, B.; Zhao, D.; Stucky, G. D. High-Yield Synthesis of Periodic Mesoporous Silica Rods and Their Replication to Mesoporous Carbon Rods. *Adv. Mater.* **2002**, *14*, 1742−1745.
(13) Yoon, S. B.; Chai, G. S.; Kang, S. K.; Yu, J. S.; Gierszal, K. P.; Jaroniec, M. Graphitized Pitch-Based Carbons with Ordered Nanopores Synthesized by Using Colloidal Crystals as Templates. *J. Am. Chem. Soc.* **2005**, *127*, 4188−4189.
(14) Jang, J.; Lim, B.; Choi, M. A Simple Synthesis of Mesoporous Carbons with Tunable Mesopores Using a Colloidal Template-Mediated Vapor Deposition Polymerization. *Chem. Commun.* **2005**, *28*, 4214−4216.
(15) Yan, Y.; Zhang, F.; Meng, Y.; Tu, B.; Zhao, D. One-Step Synthesis of Ordered Mesoporous Carbonaceous Spheres by an Aerosol-Assisted Self-Assembly. *Chem. Commun.* **2007**, *30*, 2867−2869.
(16) Kyotani, T.; Tsai, L.; Tomita, A. Formation of Ultrafine Carbon Tubes by Using an Anodic Aluminum Oxide Film as a Template. *Chem. Mater.* **1995**, *7*, 1427−1428.
(17) Li, J.; Moskovits, M.; Haslett, T. L. Nanoscale Electroless Metal Deposition in Aligned Carbon Nanotubes. *Chem. Mater.* **1998**, *10*, 1963−1967.
(18) Li, J.; Papadopoulos, C.; Xu, J.; Moskovits, M. Highly-Ordered Carbon Nanotube Arrays for Electronics Applications. *Appl. Phys. Lett.* **1999**, *75*, 367−369.
(19) Liang, C.; Dai, S. Synthesis of Mesoporous Carbon Materials *via* Enhanced Hydrogen-Bonding Interaction. *J. Am. Chem. Soc.* **2006**, *128*, 5316−5317.
(20) Liang, C.; Hong, K.; Guiochon, G. A.; Mays, J. W.; Dai, S. Synthesis of a Large-Scale Highly Ordered Porous Carbon Film by Self-Assembly of Block Copolymers. *Angew. Chem., Int. Ed.* **2004**, *43*, 5785−5789.
(21) Meng, Y.; Gu, D.; Zhang, F.; Shi, Y.; Yang, H.; Li, Z.; Yu, C.; Tu, B.; Zhao, D. Ordered Mesoporous Polymers and Homologous Carbon Frameworks: Amphiphilic Surfactant Templating and Direct Transformation. *Angew. Chem.* **2005**, *117*, 7215−7221.
(22) Zhang, F.; Meng, Y.; Gu, D.; Yan, Y.; Yu, C.; Tu, B.; Zhao, D. A Facile Aqueous Route to Synthesize Highly Ordered Mesoporous Polymers and Carbon Frameworks with Ia3d Bicontinuous Cubic Structure. *J. Am. Chem. Soc.* **2005**, *127*, 13508−13509.
(23) Mun, Y.; Jo, C.; Hyeon, T.; Lee, J.; Ha, K. S.; Jun, K. W.; Lee, S. H.; Hong, S. W.; Lee, H. I.; Yoon, S. Simple Synthesis of Hierarchically Structured Partially Graphitized Carbon by Emulsion/Block-Copolymer Co-Template Method for High Power Supercapacitors. *Carbon* **2013**, *64*, 391−402.
(24) Tang, J.; Liu, J.; Li, C.; Li, Y.; Tade, M. O.; Dai, S.; Yamauchi, Y. Synthesis of Nitrogen-Doped Mesoporous Carbon Spheres with Extra-Large Pores through Assembly of Diblock Copolymer Micelles. *Angew. Chem., Int. Ed.* **2015**, *54*, 588−593.
(25) Fang, Y.; Lv, Y.; Che, R.; Wu, H.; Zhang, X.; Gu, D.; Zheng, G.; Zhao, D. Two-Dimensional Mesoporous Carbon Nanosheets and Their Derived Graphene Nanosheets: Synthesis and Efficient Lithium Ion Storage. *J. Am. Chem. Soc.* **2013**, *135*, 1524−1530.
(26) Tian, H.; Lin, Z.; Xu, F.; Zheng, J.; Zhuang, X.; Mai, Y.; Feng, X. Quantitative Control of Pore Size of Mesoporous Carbon Nanospheres through the Self-Assembly of Diblock Copolymer Micelles in Solution. *Small* **2016**, *12*, 3155−3163.
(27) Yang, Z.; Zhang, Y.; Kong, J.; Wong, S.; Li, X.; Wang, J. Hollow Carbon Nanoparticles of Tunable Size and Wall Thickness by Hydrothermal Treatment of Cyclodextrin Templated by F127 Block Copolymers. *Chem. Mater.* **2013**, *25*, 704−710.
(28) Tan, K. W.; Jung, B.; Werner, J. G.; Rhoades, E. R.; Thompson, M. O.; Wiesner, U. Porous Materials. Transient Laser Heating Induced Hierarchical Porous Structures from Block Copolymer-Directed Self-Assembly. *Science* **2015**, *349*, 54−58.
(29) Dong, Y.; Lin, H.; Jin, Q.; Li, L.; Wang, D.; Zhou, D.; Qu, F. Synthesis of Mesoporous Carbon Fibers with a High Adsorption Capacity for Bulky Dye Molecules. *J. Mater. Chem. A* **2013**, *1*, 7391−7398.
(30) Zhong, M.; Kim, E. K.; McGann, J. P.; Chun, S. E.; Whitacre, J. F.; Jaroniec, M.; Matyjaszewski, K.; Kowalewski, T. Electrochemically Active Nitrogen-Enriched Nanocarbons with Well-Defined Morphology Synthesized by Pyrolysis of Self-Assembled Block Copolymer. *J. Am. Chem. Soc.* **2012**, *134*, 14846−14857.
(31) Tang, C.; Qi, K.; Wooley, K. L.; Matyjaszewski, K.; Kowalewski, T. Well-Defined Carbon Nanoparticles Prepared from Water-Soluble Shell Cross-Linked Micelles that Contain Polyacrylonitrile Cores. *Angew. Chem., Int. Ed.* **2004**, *43*, 2783−2787.
(32) Kruk, M.; Dufour, B.; Celer, E. B.; Kowalewski, T.; Jaroniec, M.; Matyjaszewski, K. Synthesis of Mesoporous Carbons Using Ordered and Disordered Mesoporous Silica Templates and Polyacrylonitrile as Carbon Precursor. *J. Phys. Chem. B* **2005**, *109*, 9216−9225.
(33) Kruk, M.; Dufour, B.; Celer, E. B.; Kowalewski, T.; Jaroniec, M.; Matyjaszewski, K. Well-Defined poly (ethylene oxide)-polyacrylonitrile Diblock Copolymers as Templates for Mesoporous Silicas and Precursors for Mesoporous Carbons. *Chem. Mater.* **2006**, *18*, 1417−1424.
(34) Hesse, S. A.; Werner, J. G.; Wiesner, U. One-Pot Synthesis of Hierarchically Macro-and Mesoporous Carbon Materials with Graded Porosity. *ACS Macro Lett.* **2015**, *4*, 477−482.
(35) Kosonen, H.; Ruokolainen, J.; Nyholm, P.; Ikkala, O. Self-Organized Thermosets: Blends of Hexamethyltetramine Cured Novolac with Poly (2-vinylpyridine)-*block*-poly (isoprene). *Macromolecules* **2001**, *34*, 3046−3049.
(36) Valkama, S.; Nykänen, A.; Kosonen, H.; Ramani, R.; Tuomisto, F.; Engelhardt, P.; Brinke, G.; Ikkala, O.; Ruokolainen, J. Hierarchical Porosity in Self-Assembled Polymers: Post-Modification of Block Copolymer-Phenolic Resin Complexes by Pyrolysis Allows the

DOI: 10.1021/acs.iecr.6b03048
Ind. Eng. Chem. Res. 2016, 55, 11502−11511

Control of Micro- and Mesoporosity. *Adv. Funct. Mater.* **2007**, *17*, 183−190.
(37) Hu, D.; Xu, Z.; Zeng, K.; Zheng, S. From Self-Organized Novolac Resins to Ordered Nanoporous Carbons. *Macromolecules* **2010**, *43*, 2960−2969.
(38) Huang, Y.; Cai, H.; Yu, T.; Zhang, F.; Zhang, F.; Meng, Y.; Gu, D.; Wan, Y.; Sun, X.; Tu, B. Formation of Mesoporous Carbon with A Face-Centered-Cubic Structure and Bimodal Architectural Pores from the Reverse Amphiphilic Triblock Copolymer PPO-PEO-PPO. *Angew. Chem.* **2007**, *119*, 1107−1111.
(39) Knop, A.; Scheib, W. *Chemistry and Application of Phenolic Resins*; Springer-Verlag: Berlin, 1979.
(40) Yamashita, Y.; Ouchi, K. A Study on Carbonization of Phenol-formaldehyde Resin Labelled with Deuterium and 13C. *Carbon* **1981**, *19*, 89−94.
(41) Fyfe, C. A.; McKinnon, M. S.; Rudin, A.; Tchir, W. J. Investigation of the Mechanism of the Thermal Decomposition of Cured Phenolic Resins by High-Resolution Carbon-13 CP/MAS Solid-State NMR Spectroscopy. *Macromolecules* **1983**, *16*, 1216−1219.
(42) Zhang, X.; Solomon, D. H. Carbonization Reactions in Novolac Resins, Hexamethylenetetramine, and Furfuryl Alcohol Mixtures. *Chem. Mater.* **1999**, *11*, 384−391.
(43) Meng, Y.; Gu, D.; Zhang, F.; Shi, Y.; Cheng, L.; Feng, D.; Wu, Z.; Chen, Z.; Wan, Y.; Stein, A.; Zhao, D. A Family of Highly Ordered Mesoporous Polymer Resin and Carbon Structures from Organic-Organic Self-Assembly. *Chem. Mater.* **2006**, *18*, 4447−4464.
(44) Zhang, F.; Meng, Y.; Gu, D.; Yan, Y.; Yu, C.; Tu, B.; Zhao, D. A Facile Aqueous Route to Synthesize Highly Ordered Mesoporous Polymers and Carbon Frameworks with Ia3d Bicontinuous Cubic Structure. *J. Am. Chem. Soc.* **2005**, *127*, 13508−13509.
(45) Huang, Y.; Cai, H.; Yu, T.; Zhang, F.; Zhang, F.; Meng, Y.; Gu, D.; Wan, Y.; Sun, X.; Tu, B.; Zhao, D. Formation of Mesoporous Carbon with a Face-Centered-Cubic Fd3m Structure and Bimodal Architectural Pores from the Reverse Amphiphilic Triblock Copolymer PPO-PEO-PPO. *Angew. Chem.* **2007**, *119*, 1107−1111.
(46) Deng, Y.; Cai, Y.; Sun, Z.; Gu, D.; Wei, J.; Li, W.; Guo, X.; Yang, J.; Zhao, D. Controlled Synthesis and Functionalization of Ordered Large-Pore Mesoporous Carbons. *Adv. Funct. Mater.* **2010**, *20*, 3658−3665.
(47) Deng, Y.; Yu, T.; Wan, Y.; Shi, Y.; Meng, Y.; Gu, D.; Zhang, L.; Huang, Y.; Liu, C.; Wu, X.; Zhao, D. Ordered Mesoporous Silicas and Carbons with Large Accessible Pores Templated from Amphiphilic Diblock Copolymer Poly(ethylene oxide)-*b*-polystyrene. *J. Am. Chem. Soc.* **2007**, *129*, 1690−1697.
(48) Li, J.; Kuo, S. Phase Behavior of Mesoporous Nanostructures Templated by Amphiphilic Crystalline-Crystalline Diblock Copolymers of Poly(ethylene oxide-*b*-ε-caprolactone). *RSC Adv.* **2011**, *1*, 1822−1833.
(49) Li, J.; Lin, Y.; Kuo, S. From Microphase Separation to Self-organized Mesoporous Phenolic Resin through Competitive Hydrogen Bonding with Double-Crystalline Diblock Copolymers of Poly(ethylene oxide-*b*-ε-caprolactone). *Macromolecules* **2011**, *44*, 9295−9309.
(50) Rebizant, V.; Venet, A. S.; Tournilhac, F.; Girard-Reydet, E.; Navarro, C.; Pascault, J. P.; Leibler, L. Chemistry and Mechanical Properties of Epoxy-Based Thermosets Reinforced by Reactive and Nonreactive SBMX Block Copolymers. *Macromolecules* **2004**, *37*, 8017−8027.
(51) Zhu, M.; Wei, L.; Li, M.; Jiang, L.; Du, F.; Li, Z.; Li, F. A Unique Synthesis of a Well-defined Block Copolymer Having Alternating Segments Constituted by Maleic Anhydride and Styrene and the Self-Assembly Aggregating Behavior Thereof. *Chem. Commun.* **2001**, *4*, 365−366.
(52) De Brouwer, H.; Schellekens, M. A.; Klumperman, B.; Monteiro, M. J.; German, A. L. Controlled Radical Copolymerization of Styrene and Maleic Anhydride and the Synthesis of Novel Polyolefin-Based Block Copolymers by Reversible Addition-fragmentation Chain-Transfer (RAFT) Polymerization. *J. Polym. Sci., Part A: Polym. Chem.* **2000**, *38*, 3596−3603.
(53) Chernikova, E.; Terpugova, P.; Bui, C.; Charleux, B. Effect of Comonomer Composition on the Controlled Free-Radical Copolymerization of Styrene and Maleic Anhydride by Reversible Addition-fragmentation Chain Transfer (RAFT). *Polymer* **2003**, *44*, 4101−4107.
(54) Lai, J. T.; Filla, D.; Shea, R. Functional Polymers from Novel Carboxyl-Terminated Trithiocarbonates as Highly Efficient RAFT Agents. *Macromolecules* **2002**, *35*, 6754−6756.
(55) Yu, R.; Zheng, S. Polystyrene-block-Polybutadiene-block-Polystyrene Triblock Copolymer Meets Silica: From Modification of Copolymer to Formation of Mesoporous Silica. *Ind. Eng. Chem. Res.* **2015**, *54*, 6454−6466.
(56) Seymour, R. B.; Garner, D. P. Relationship of Temperature to Composition of Copolymers of Methylstyrene and Maleic Anhydride. *Polymer* **1976**, *17*, 21−24.
(57) Ebdon, J. R.; Towns, C. R. On the Role of Monomer-Monomer Complexes in Alternating Free-Radical Copolymerizations: the Case of Styrene and Maleic Anhydride. *J. Macromol. Sci., Polym. Rev.* **1986**, *26*, 523−550.
(58) Henry, S. M.; Elsayed, M. E.; Pirie, C. M.; Hoffman, A. S.; Stayton, P. S. pH-Responsive Poly(styrene-*alt*-maleic anhydride) Alkylamide Copolymers for Intracellular Drug Delivery. *Biomacromolecules* **2006**, *7*, 2407−2414.
(59) Feng, X.; Pan, C. Synthesis of Amphiphilic Miktoarm ABC Star Copolymers by RAFT Mechanism using Maleic Anhydride as Linking Agent. *Macromolecules* **2002**, *35*, 4888−4893.
(60) Tarazona, P. Free-Energy Density Functional for Hard Spheres. *Phys. Rev. A: At., Mol., Opt. Phys.* **1985**, *31*, 2672−2679.
(61) Telo da Gama, M. M.; Gubbins, K. Adsorption and Orientation of Amphiphilic Molecules at a Liquid-Liquid Interface. *Mol. Phys.* **1986**, *59*, 227−239.
(62) Occelli, M. L.; Olivier, J. P.; Petre, A.; Auroux, A. Determination of Pore Size Distribution, Surface Area, and Acidity in Fluid Cracking Catalysts (FCCS) from Nonlocal Density Functional Theoretical Models of Adsorption and from Microcalorimetry Methods. *J. Phys. Chem. B* **2003**, *107*, 4128−4136.

DOI: 10.1021/acs.iecr.6b03048
Ind. Eng. Chem. Res. 2016, 55, 11502−11511